Microfluid Nanofluid (2015) 18:1365–1371
DOI 10.1007/s10404-014-1535-3

RESEARCH PAPER

Molecular free paths in nanoscale gas flows

Murat Barisik · Ali Beskok

Received: 15 July 2014 / Accepted: 8 December 2014 / Published online: 16 December 2014

Abstract Average distance traveled by gas molecules between intermolecular collisions, known as the mean free path (MFP), is a key parameter for characterizing gas flows in the entire Knudsen regime. Recent literature presents variations in MFP as a function of the surface confinement, which is in disagreement with the kinetic theory and leads to wrong physical interpretations of nanoscale gas flows. This controversy occurs due to erroneous definition and calculation practices, such as consideration of gas wall collisions, using local bins smaller than a MFP, and utilizing time frames shorter than a mean collision time in the MFP calculations. This study reports proper molecular MFP calculations in nanoscale confinements by using realistic molecular surfaces. We utilize molecular dynamics (MD) simulations to calculate gas MFP in three-dimensional periodic systems of various sizes and for force-driven gas flows confined in nano-channels. Studies performed in the transition flow regime in various size nano-channels and under a range of gas–surface interaction strengths have shown isotropic mean travelled distance and MFP values in agreement with the kinetic theory regardless of the surface forces and surface adsorption effects. Comparison of the velocity profiles obtained in MD simulations with the linearized Boltzmann solutions at predicted Knudsen values shows good agreement in the bulk of the channels, while deviations in the near wall region due to the influence of surface forces are reported.

M. Barisik
Mechanical Engineering Department,
Izmir Institute of Technology, Izmir 35430, Turkey

A. Beskok (✉)
Mechanical Engineering Department, Southern Methodist University, Dallas, TX 75275-0337, USA
e-mail: abeskok@smu.edu

Keywords Rarefied gas dynamics · Transition flow regime · Molecular surface force effects · Molecular dynamics

1 Introduction

Gas states evolve through intermolecular collisions separated by ballistic motion of molecules characterized by the molecular free paths. The average of these, known as the mean free path (MFP, λ), is a key parameter in gas dynamics. Non-equilibrium behavior in rarefied (low-density), microscale, and nanoscale gas flows is determined as a function of the Knudsen number (Kn), which is the ratio of gas MFP and the characteristic flow dimension. While the channel height determines the characteristic dimension for fully developed internal flows, accurate prediction of Kn relies on correct calculation of MFP. Recent literature claims spatial variations of MFP in scales smaller than λ with gradients normal to the channel surfaces (Arlemark and Reese 2009; Dongari et al. 2011a, b, 2013a; Prabha et al. 2013; Qixin and Zhiyong 2014). In addition, confinement size-dependent MFP models have been developed to define an effective viscosity (Arlemark et al. 2010; Dongari et al. 2011b, 2013a, b; Dongari and Agrawal 2012; Guo et al. 2007; Peng et al. 2004) and a corresponding phoretic velocity (Dongari et al. 2010) in the derivation of extended Navier–Stokes equations. Further investigations of these new findings and enhanced understanding of nanoscale confined gas flows are crucial for progress in vast applications, including the development of nano-engineered composite membranes for separation/storage of gas molecules (Furukawa and Yaghi 2009; Venna and Carreon 2009; Yave et al. 2010) and for modeling gas recovery from nano-porous shale reservoirs (Civan 2010, 2011; Loucks et al. 2009).

Kinetic theory definition of MFP (λ_{KT}) for hard sphere gas molecules is given as (Karniadakis et al. 2005)

$$\lambda_{KT} = \frac{1}{\sqrt{2}\pi\sigma_{HS}^2 n} \tag{1}$$

where n is the local number density, and σ_{HS} is the molecular diameter. This derivation involves gas–gas interactions only. Therefore, sampled gas molecules do not go through gas–surface collisions. Alternatively, one can use the kinetic theory definition of viscosity for hard sphere molecules (μ) and employ gas density (ρ) and temperature (T) to arrive at

$$\lambda_{KT} = \frac{\sqrt{\pi}\mu}{\rho\sqrt{RT}}, \tag{2}$$

where R is the specific gas constant.

Mean free path of gas molecules can also be calculated using molecular dynamics (MD). For this purpose, we use monatomic gas molecules going through van der Waals interactions modeled by the truncated Lennard-Jones (LJ) 6–12 potential. We simulate argon molecules with molecular mass of $m_{Ar} = 6.63 \times 10^{-26}$ kg and diameter of $\sigma_{LJ,\,Ar} = 0.3405$ nm. Depth of the potential well is $\varepsilon_{Ar} = 119.8 \times k_b$, where k_b is the Boltzmann constant. We used a cutoff distance of $r_c = 1.08$ nm, which is approximately equal to 3.17 σ_{LJ} for argon molecules. At this cutoff distance, attractive part of the LJ potential is reduced to 0.00392ε. During simulations, argon–argon interactions use ε_{Ar}, while argon–wall interactions use ε_{Ar}, 2 ε_{Ar}, and 3 ε_{Ar} to investigate increasing wall attraction. Walls were modeled molecularly using face-centered cubic (FCC) structure with (1,0,0) plane facing the gas. For simplicity, molecular diameters of wall molecules are assumed to be equivalent to that of argon. We present our results as a function of normalized interaction parameters, which result in $\varepsilon_{ff} = 1$ for gas–gas and $\varepsilon_{wf}/\varepsilon_{ff} = 1$, 2, and 3 for gas–wall interactions.

Using MD, we measured the total distance traveled by every molecule to calculate a mean travelled distance (MTD) as,

$$\mathrm{MTD} = \sum_{j=1}^{m}\left(\frac{1}{N}\sum_{i=1}^{N}\left((t_j - t_{j-1}) \times \left|u^i(t_j)\right| + \frac{1}{2} \times (t_j - t_{j-1})^2 \times \left|a^i(t_j)\right|\right)\right), \tag{3}$$

where $u^i(t_j)$ and $a^i(t_j)$ are the velocity and acceleration of molecule i at time t_j; N is the total number of molecules in the system, and m is the total number of time steps during the measurements. MTD in x-, y-, and z-directions is also measured separately to investigate its isotropy in nanoscale confinements.

The MFP calculation requires additional attention to record the free paths of individual molecules and counting the number of collision events. The latter requires collision diameter, which cannot be defined conventionally for molecules interacting via LJ potential. Using local thermodynamic state of argon gas and its corresponding bulk viscosity, we calculated MFP using Eq. (2). Equating this value to λ_{KT} in Eq. (1), we obtained a collision diameter, σ_{col}, for argon as $1.06 \times \sigma_{LJ,Ar}$. We define collision events as two argon molecules getting close to each other to a distance of σ_{col}. Since the molecules interact via LJ potential, any two gas molecules can remain close to each other for some finite time before they repel each other. We count these events as a single collision in our analyzes. For free path measurements, one should record MTDs of each molecule except during the collision events. MTD measurements should be performed in a time frame proportional to the mean collision time.

MD simulations start with the Maxwell–Boltzmann velocity distribution of gas molecules at 298 K. Initial particle distribution is evolved 10^6 time steps (4 ns) to reach an isothermal steady state using 4 fs (~0.002 τ) time steps, after which 2×10^6 time steps (40 ns) are performed for time averaging. Canonical ensemble is performed by utilizing the Nose–Hoover thermostat (Evans and Hoover 1986).

We first analyze three-dimensional systems in a periodic box of various dimensions by simulating argon gas at three different densities corresponding to the ideal gas state. Without any surface effects, these sets of simulations are designed to test our MFP calculation algorithm at different densities and simulation domain sizes. Table 1 shows three different domain sizes used for each density case along with the number of gas molecules used in the simulations, gas density, λ_{KT} from Eq. (2), MTD in three mutually orthogonal dimensions, total MTD, MD calculated mean molecular speed $\bar{c}_{MD}$, and λ_{MD}. The MTD values are measured using Eq. (3) with 4-ns simulation intervals. Results in Table 1 are the average of ten 4-ns sampled values. We calculated the mean molecular speed using $\bar{c}_{MD} = \mathrm{MTD}/\Delta t$. Results show great agreement with kinetic theory predictions given by $\bar{c} = \sqrt{8RT/\pi}$, which is ~397 m/s for argon gas at 298 K. MTD values measured in each direction show isotropy of the system. MFP from MD calculations matches kinetic theory predictions very accurately, proving no size effects of domain periodicity. Based on this observation, we conclude that MD can predict MFP properly in periodic systems that are about λ long or larger.

Next, we simulate force-driven argon gas flows between molecularly modeled two parallel surfaces separated with a distance H. Periodic boundary conditions are applied in the stream wise and lateral directions. Size of the domain is crucial, especially in the flow direction to simulate the correct gas thermodynamic state. Based on previous results, simulation domains are designed to span ~λ_{Ar} or more in the periodic directions in order to capture gas–gas intermolecular collisions and to calculate the MFP properly. Large

Table 1 MD simulation parameters and measured MTD and MFP values with kinetic theory predictions in periodic rectangular domains

Dimensions (nm)	# Gas molecules	Density (kg/m^3)	λ_{KT} (nm)	MTD_x (nm) in 4 ns	MTD_y (nm) in 4 ns	MTD_z (nm) in 4 ns	MTD (nm) in 4 ns	$\bar{c}_{MD}$ (m/s)	λ_{MD} (nm)
27 × 27 × 27	2,250	3.761	30.3	791.5	790.1	791.5	1,584.1	396.03	30.8
54 × 54 × 54	9,000	3.761	30.3	791.1	791.4	790.8	1,583.8	395.96	30.7
108 × 108 × 108	20,250	3.761	30.3	790.9	790.6	791.2	1,584.9	396.23	30.4
54 × 54 × 54	4,500	1.887	60.3	794.4	789.3	788.9	1,583.9	395.97	60.9
108 × 108 × 108	18,000	1.887	60.3	790.2	792.4	788.6	1,585.1	396.28	61.4
162 × 162 × 162	40,500	1.887	60.3	793.7	790.5	793.4	1,584.3	396.10	60.7
108 × 108 × 108	9,000	0.944	120.5	796.6	788.4	792.1	1,585.3	396.33	121.5
216 × 216 × 216	36,000	0.944	120.5	790.2	792.9	789.3	1,584.5	396.13	122.3

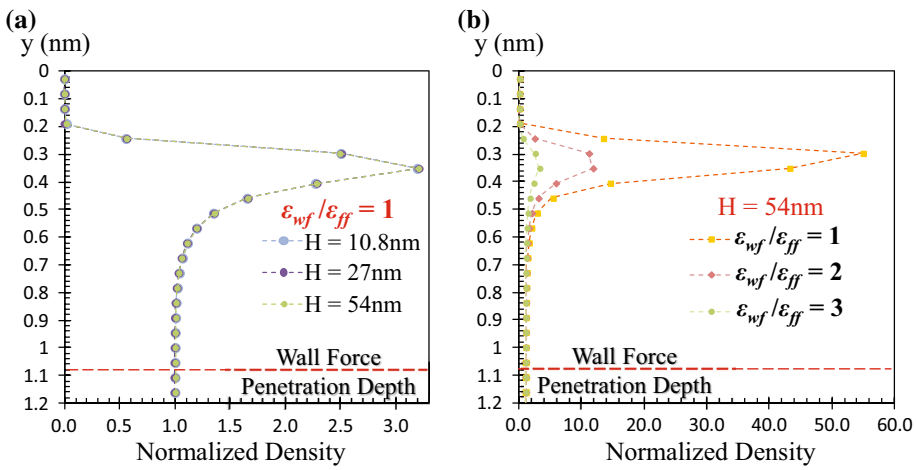

Fig. 1 Normalized gas density distributions in the near wall region for 10.8, 27, and 54 nm height channels for $\varepsilon_{wf}/\varepsilon_{ff} = 1$. Normalization is obtained using the bulk channel density **(a)**. Normalized gas density in 54 nm height channels for gas–wall interaction parameters of $\varepsilon_{wf}/\varepsilon_{ff} = 1$, 2, and 3 **(b)**

domain sizes greatly complicate classical MD simulations, where the number of wall molecules overwhelms the simulation. We addressed this computational difficulty by using the Smart Wall Molecular Dynamics (SWMD) algorithm (Barisik et al. 2010). For three-dimensional FCC crystal structured walls used here, the SWMD limits memory use of a semi-infinite wall slab into a stencil of 74 wall molecules. Current SWMD is a fixed lattice model, where wall molecules are rigid and keep their corresponding FCC positions (i.e., cold wall model). When a gas molecule approaches the surface and enters the near wall region, the SWMD wall stencil models presence of a semi-infinite wall.

Argon gas density is varied to obtain $k = 1$ flows $[k = (\sqrt{\pi}/2)Kn]$ in 10.8, 27, and 54 nm height channels. In linearized Boltzmann solutions, k is frequently used as the modified Knudsen number. A constant driving force (F_{drive}) is applied on each gas molecule in the stream wise direction, while the applied force is specified according to the flow area. Specifically, F_{drive} is adjusted to create low Mach number gas flows ($M \approx 0.07$) to maintain isothermal and nearly incompressible flow conditions in all cases. For this purpose, F_{drive} is fixed at 20.2×10^{-15} N/atom in the 10.8 nm height channel (10.8 nm × 54 nm × 54 nm system) and 8.08×10^{-15} N/atom in the 27 nm height channel (27 nm × 54 nm × 54 nm system), while the 54-nm channel cases (54 nm × 54 nm × 54 nm system) use $F_{drive} = 4.04 \times 10^{-15}$ N/atom. Local gas temperature is carefully monitored to ensure isothermal conditions throughout the channels.

In order to investigate the effects of gas–wall interactions, we simulate $\varepsilon_{wf}/\varepsilon_{ff} = 1$, 2, and 3 cases for gas flows in 54 nm height channel, while simulations for 10.8 and 27 nm height channels are performed for $\varepsilon_{wf}/\varepsilon_{ff} = 1$. Figure 1 shows density distribution within 1.2 nm from the walls. Using the LJ cutoff distance, van der Walls forces from the walls penetrate approximately 1.08 nm from each surface, and this region is identified as the *wall force penetration depth* (L_f) (Barisik et al. 2010; Barisik and Beskok 2010, 2011a, b, 2012, 2014). Regardless of the channel height and the local thermodynamic state, density profiles near the walls normalized by the bulk flow density show a peak within ~0.4 nm from the center of wall molecules ($y = 0$). This density increase was shown earlier in (Barisik and Beskok 2011a, b). Match in the density profiles in Fig. 1a is simply due to the identical gas–surface coupling used in

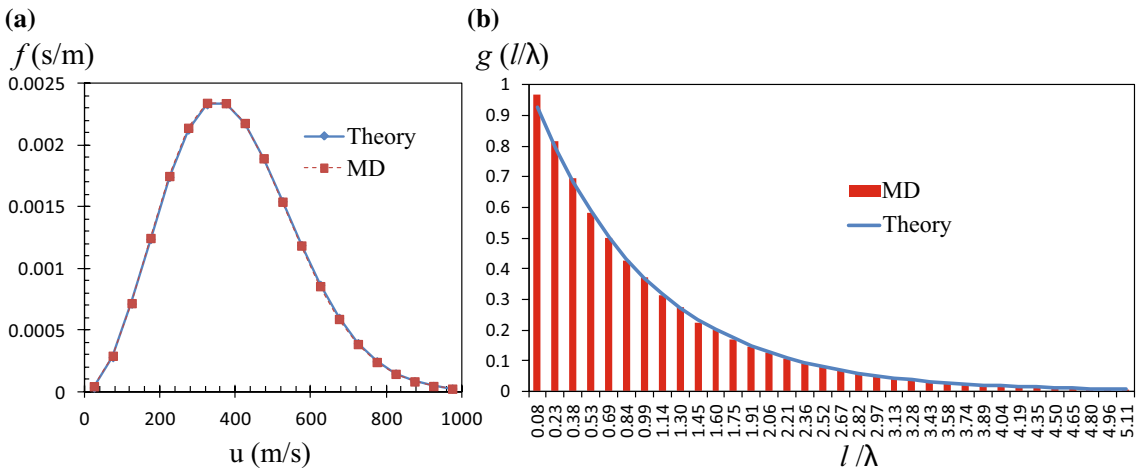

Fig. 2 Velocity distribution of argon gas at 298 K confined in nano-channels calculated by MD and predicted by Maxwell–Boltzmann distribution **(a)**. Distribution of normalized gas free paths measured by MD and predicted by kinetic theory **(b)**

Table 2 MD simulation parameters and measured MTD and MFP values with kinetic theory predictions for force-driven nano-channel flows

Height (nm)	$\varepsilon_{wf}/\varepsilon_{ff}$	Density (kg/m^3)	λ_{KT} (nm)	MTD_x (nm) in 4 ns	MTD_y (nm) in 4 ns	MTD_z (nm) in 4 ns	MTD (nm) in 4 ns	$\bar{c}$ (m/s)	λ_{MD} (nm)	Kn_{MD}	k_{MD}
10.8	1	9.291	12.2	790.9	791.9	790.6	1,582.4	395.61	12.5	1.16	1.02
27	1	3.761	30.3	790.1	792.3	791.6	1,585.1	396.28	30.8	1.14	1.00
54	1	1.887	60.3	791.8	790.6	790.4	1,585.7	396.43	60.9	1.13	1.01
54	2	1.887	60.3	790.9	791.2	792.3	1,584.4	396.1	61.5	1.14	1.01
54	3	1.887	60.3	791.3	792.5	791.4	1,585.5	396.4	61.3	1.14	1.01

these cases (i.e., $\varepsilon_{wf}/\varepsilon_{ff} = 1$). Density distributions near the wall for different $\varepsilon_{wf}/\varepsilon_{ff}$ values are shown in Fig. 1b. Increasing the surface force increases particle residence time in the near wall region and eventually leads to gas adsorption. Since different $\varepsilon_{wf}/\varepsilon_{ff}$ values result in different number of adsorbed molecules on the surfaces, we start each simulation using the proper number of molecules to obtain the desired gas density in the bulk of the channels. This is important to keep *Kn* a constant. Although the density profiles in Fig. 1b are obtained for force-driven gas flows, our earlier work on shear-driven gas flows has shown similar density profiles with variation of $\varepsilon_{wf}/\varepsilon_{ff}$ (Barisik and Beskok 2012). Results show that the near wall density profile is determined by the gas–surface interaction parameter, and it is independent of the local *Kn*.

In order to properly characterize the nanoscale confinement effects, we first computed the velocity distribution of gas molecules and compared these with Maxwell–Boltzmann velocity distribution at 298 K. Regardless of the channel height, density, surface potential, and flow conditions, MD gas velocity distribution is found identical to the kinetic theory description, which shows that *local thermal equilibrium* is maintained for these isothermal cases regardless of the nanoscale confinement effects induced by molecular surfaces (Fig. 2a).

Table 2 shows MTD values in three mutually orthogonal directions (*y* is the wall normal direction), MTD, mean molecular speed, MFP, and *Kn* values obtained by MD simulations for various height nano-channels and under different gas–wall interaction parameters. All these parameters match with kinetic theory-based predictions. Similar to the periodic system results, MTDs in different directions are isotropic. Collision frequencies of gas molecules show large variations inside the wall force penetration region as a function of the surface interaction potential. In definition of the MFP, counting the number of gas–gas collisions in the near wall region leads to wrong assessments due to the adsorbed gas molecules. Interestingly enough, MTD values measured in the entire domain are not affected by the near wall region. Calculations of MTD and gas–gas collision frequency outside the force penetration depth result in MFP values that agree very well with the kinetic theory predictions. Distribution of the molecular free paths of gas molecules (l) is shown in Fig. 2b. MD results normalized with the corresponding mean free paths match $g(l/\lambda) = e^{-l/\lambda}$, provided by the kinetic theory (Goodman and Wachman 1976).

Having established these key results, let us look into the sources of errors in MFP calculations in the literature. MFP is the average distance traveled by molecules between intermolecular collisions. Given this fact, the first common cause of error is counting of the gas–wall collisions in determination of λ (Arlemark et al. 2010; Arlemark and Reese 2009; Dongari et al. 2010, 2011a, b, 2013a, b; Dongari and Agrawal 2012; Guo et al. 2007; Peng et al. 2004; Prabha et al. 2013; Qixin and Zhiyong 2014). In the case of gas adsorption on the surface, gas molecules will collide with immobilized gas molecules on the surface. Such gas–gas collisions should also be excluded, since adsorbed gas molecules are not free to move.

Second, we look into literature that reports time-dependent variations in the MFP (Arlemark and Reese 2009; Dongari et al. 2011a). Starting from a system in thermodynamic equilibrium, one can start calculating the MFP as a function of time. Due to the presence of diverse gas free paths in the system, one will first observe smaller free paths. Only after a considerable amount of time, the system will exhibit all free paths in the spectra shown in Fig. 2b, and the MFP will converge to the value predicted by kinetic theory. Simply stated, time-dependent MFP results are solely due to the simulation times being smaller than the mean collision time. One can avoid this mistake by averaging the results for much longer times than the mean collision time.

The third common error is utilization of free paths bounded by the channel height, for derivation of an effective viscosity for extended Navier–Stokes equations (Arlemark et al. 2010; Dongari et al. 2010, 2011a, 2013a, b; Dongari and Agrawal 2012; Guo et al. 2007; Peng et al. 2004). This approach makes fluid viscosity a function of the channel height. Although the largest gas free path for rarefied gas confined in a sphere is bounded by the sphere's diameter, gas-free paths in other geometries can exhibit free paths longer than the geometric dimensions, since molecules going through intermolecular collisions scatter in every direction. Results in Fig. 2b prove that gas free paths confined in a nano-size slit exhibits the entire spectrum predicted by the kinetic theory. This outcome brings an additional criticism to the concept of "effective viscosity." Since our results are in concurrence with Eq. (2), gas viscosity in the nano-confined system must also be a constant and determined by the local thermodynamic state. Given these facts, validity of the extended Navier–Stokes equations becomes questionable.

The forth common error is in reporting spatial variations of MPF due to the confinement effects (Arlemark and Reese 2009; Dongari et al. 2011a, b, 2013a; Prabha et al. 2013; Qixin and Zhiyong 2014). Local MFP variations are physically admissible only if there are local density and temperature variations in the system, which is common in the streamwise direction for pressure driven gas flows in a channel. For $k = 1$ flows shown in Fig. 1, gas density for isothermal flow is constant outside the wall force penetration depth, and MD calculations show constant MFP. Probable causes of erroneous MFP variations across the channel are (1) utilization of time averaging smaller than the mean collision time and (2) counting of gas–wall collisions. The former cause of error is dependent on the molecular free path distribution experienced in the bins. In other words, manifestation of the same error that led to the time-dependent MFP values. The latter cause of error is induced by counting of gas–wall collisions, where bins closer to the surface could be seem experiencing different free path values due to their proximity to the walls. Such presentations are greatly unphysical and illogical. Since MFP in a nanoscale confinement is often much larger than the channel height, computational bins that are only a few angstroms thick cannot exhibit spatial variations of the MFP, since the bin size is much smaller than the mean distance travelled by gas molecules between their collisions.

An important part of this study is validation of MFPs and Knudsen numbers calculated by MD simulations by examining the local velocity profiles. For this purpose, we computed the velocity profiles for all $k = 1$ flows in different nano-confinements. Velocity profiles in the half of the channels are plotted in Fig. 3. We compared the velocity distribution with the predictions of the linearized Boltzmann equation solutions and the velocity profiles approximated by Beskok and Karniadakis Model (BKM) (Beskok and Karniadakis 1999).

Figure 3a shows the velocity profiles for $k = 1$ flows in different height channels for $\varepsilon_{wf}/\varepsilon_{ff} = 1$. Same surface configuration was studied in our earlier work on shear-driven gas flows, where the tangential momentum accommodation coefficient (TMAC, α) for this surface/gas couple at $\varepsilon_{wf}/\varepsilon_{ff} = 1$ was calculated as $\alpha = 0.75$ (Barisik and Beskok 2011b). In that study, we also validated TMAC values to be independent of the channel height, gas density, and Knudsen number. Velocity profiles based on the Boltzmann equation solutions are available in the literature for $\alpha = 1$ (Ohwada et al. 1989), while mass flow rate data for $\alpha = 0.75$ exist at various Kn values (Sharipov 2001). In order to obtain a dimensional value for the desired theoretical velocity profiles, we utilized BKM for velocity shape and obtained the magnitude of the channel averaged velocity using Boltzmann solutions in (Sharipov 2001). Results in Fig. 3a show good agreements between the MD data and predictions of the BKM away from the walls. Since the velocity profiles are presented as a function of y/H, influence of the near wall region varies with the channel height. Different than the kinetic theory and BKM, MD further considers nanoscale effects like surface forces and surface adsorption of gas molecules in addition to gas rarefaction. Nearly, parabolic velocity profiles are observed in

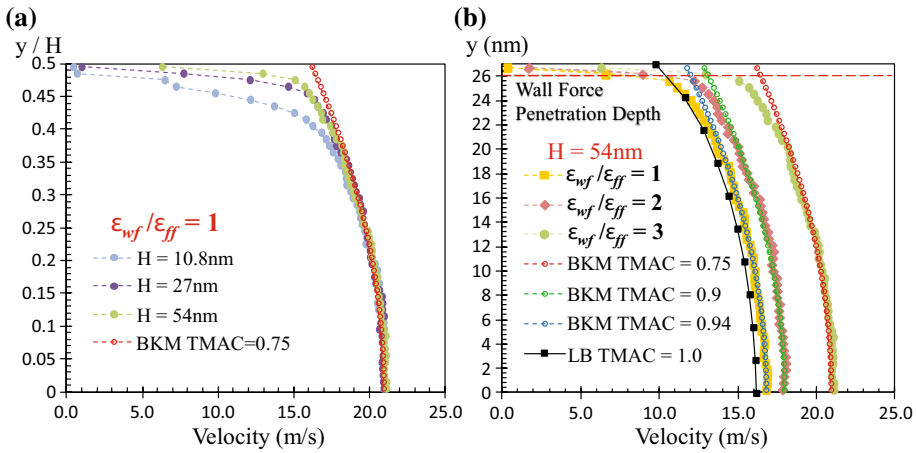

Fig. 3 MD velocity profiles for $k = 1$ flows **(a)** in 10.8, 27, and 54 nm height channels with $\varepsilon_{wf}/\varepsilon_{ff} = 1$ and **(b)** in 54 nm height channel with $\varepsilon_{wf}/\varepsilon_{ff} = 1$, $\varepsilon_{wf}/\varepsilon_{ff} = 2$, and $\varepsilon_{wf}/\varepsilon_{ff} = 3$ (*solid symbols*). Linearized Boltzmann solution for TMAC = 1 (Ohwada et al. 1989) (*solid symbol* with *solid line*), and predictions of BKM (Beskok and Karniadakis 1999) for TMAC = 0.94, 0.9, and 0.75 (*hollow symbols*) are given for comparisons

bulk of the channels with significant variations in the near wall region (i.e., within the wall force penetration length, L_f) (Barisik and Beskok 2014). Since the dimension of the near wall region remains a constant, its influence on flow physics becomes increasingly significant with decreased channel height, H. In our previous studies, we defined a new dimensionless parameter $B = L_f/H$ to characterize the nanoscale confinement effects on gas transport. Surface effects are negligible for $B \to 0$, but the near wall physics becomes dominant for finite values of B where transport behavior is completely different than the kinetic theory predictions (Barisik and Beskok 2014).

Velocity profiles for different surface interaction strengths in 54 nm channel are plotted in Fig. 3b. Our earlier work on shear-driven flows resulted in $\alpha = 0.75$, 0.9, and 0.94 for $\varepsilon_{wf}/\varepsilon_{ff} = 1$, 2, and 3, respectively (Barisik and Beskok 2012). Theoretical results are plotted using linearized Boltzmann solution at $\alpha = 1$ and using BKM and Boltzmann flow rate data for $\alpha = 0.75$. BKM velocity profiles for $\alpha = 0.9$ and 0.94 were obtained using the channel averaged velocities calculated form MD simulations. Increase in surface interaction strength leads to stronger coupling between the gas and surface atoms, which results in higher TMAC values that reduce the gas velocity and mass flow rate. In all cases, the velocity profiles in bulk of the channel match kinetic theory predictions at the corresponding Kn values. This proves that the kinetic description of Kn is applicable for nanoscale confined gas flows for $B \to 0$. Such results would be impossible if the MFP varies across the channels as claimed in recent literature.

2 Conclusions

Current claims of MFP variation normal to the nano-channel surfaces as a function of the confinement level are false. Consideration of gas–wall collisions creates a channel height dependent MFP. In addition, calculations performed in time frames shorter than a mean collision time result in time dependency of MFP. Moving one step further, our simulations employed molecular surfaces with atomistic corrugations and surface forces different than the earlier studies using Maxwell type planar boundary conditions. Even in such a case, carefully conducted MD simulations validate the kinetic theory definition of MFP in nanoscale confinements as small as 10 nm. In fact, MFP calculations should solely rely on gas–gas collisions outside the adsorbed gas regions and should be performed for a time frame that is several mean collision time long. Since MFP is a discrete length scale, it should not be measured every time step and for length scales smaller than itself. This methodology and our MFP results are validated by the velocity profiles for force-driven nano-channel flows, which agree well with the kinetic theory predictions in the bulk flow region using the Knudsen number calculated from the MFP results of MD simulations. Flow physics in the near wall region is determined by the surface force field, as previously explained in (Barisik et al. 2010; Barisik and Beskok 2010, 2011a, b, 2012, 2014).

Acknowledgments Dr. Beskok would like to thank American Chemical Society (ACS) for support under the grant number 54562-ND9.

References

Arlemark EJ, Reese JM (2009) Investigating the effects of solid boundaries on the gas mean-free-path. In: ASME 7th International Conference on Nanochannels, Microchannels, and Minichannels

Arlemark EJ, Dadzie SK, Reese JM (2010) An extension to the Navier–Stokes equations to incorporate gas molecular collisions with boundaries. J Heat Transf 132:1–041006

Barisik M, Beskok A (2010) MD simulations of nano-scale gas flows: a case study of couette flow at $Kn = 10$. In: Proceedings of the 27th Symposium on Rarefied Gas Dynamics Pacific Grove, CA, vol. 1333, p. 707

Barisik M, Beskok A (2011a) Equilibrium molecular dynamics studies on nanoscale-confined fluids. Microfluid Nanofluidics 11:269

Barisik M, Beskok A (2011b) Molecular dynamics simulations of shear driven gas flows in nano-chan. Microfluid Nanofluidics 11:611

Barisik M, Beskok A (2012) Surface-gas interaction effects on nanoscale gas flows. Microfluid Nanofluidics 13:789

Barisik M, Beskok A (2014) Scale effects in gas nano flows. Phys Fluids 26:052003

Barisik M, Kim B, Beskok A (2010) Smart wall model for molecular dynamics simulations of nanoscale gas flows. Commun Comput Phys 7:977

Beskok A, Karniadakis GE (1999) A model for flows in channels, pipes and ducts at micro and nano scales. Microscale Thermophys Eng 3(1):43–77

Civan F (2010) Effective correlation of apparent gas permeability in tight porous media. Transp Porous Media 82(2):375–384

Civan F (2011) Porous media transport phenomena. Wiley, Hoboken, New Jersey

Dongari N, Agrawal A (2012) Modeling of Navier–Stokes equations for high Knudsen number gas flows. Int J Heat Mass Transf 55:4352–4358

Dongari N, Durst F, Chakraborty S (2010) Predicting microscale gas flows and rarefaction effects through extended Navier–Stokes–Fourier equations from phoretic transport considerations. Microfluid Nanofluid 9:831

Dongari N, Zhang Y, Reese JM (2011a) Molecular free path distribution in rarefied gases. J Phys D Appl Phys 44(12):125502

Dongari N, Zhang Y, Reese JM (2011b) Modelling of Knudsen layer effects in micor/nanoscale gas flows. J Fluids Eng 133:1–071101

Dongari N, Barber RW, Emerson DR, Stefanov SK, Zhang Y, Reese JM (2013a) The effects of Knudsen Layers on rarefied cylindrical Couette gas flows. Microfluid Nanofluid 14:31

Dongari N, White C, Scanlon TJ, Zhang Y, Reese JM (2013b) Effects of curvature on rarefied gas flows between rotating concentric cylinders. Phys Fluids 25:052003

Evans DJ, Hoover WG (1986) Flows far from equilibrium via molecular-dynamics. Annu Rev Fluid Mech 18:243–264

Furukawa H, Yaghi OM (2009) Storage of hydrogen, methane, and carbon dioxide in highly porous covalent organic frameworks for clean energy applications. J Am Chem Soc 131(25):8875–8883

Goodman FO, Wachman HY (1976) Dynamics of gas-surface scattering. Academic Press, New York

Guo ZL, Shi BC, Zheng CG (2007) An extended Navier–Stokes formulation for gas flows in the Knudsen layer near a wall. EPL (Europhys Lett) 80:24001

Karniadakis GE, Beskok A, Aluru N (2005) Micro flows and nano flows: fundamentals and simulation. Springer, New York

Loucks RG, Reed RM, Ruppel SC, Jarvie DM (2009) Morphology, genesis, and distribution of nanometer-scale pores in siliceous mudstones of the Mississippian Barnett Shale. J Sediment Res 79(12):848–861

Ohwada T, Sone Y, Aoki K (1989) Numerical analysis of the Poiseuille and thermal transpiration flows between two parallel plates on the basis of the Boltzmann equation for hard-sphere molecules. Phys Fluids A 1:2042

Peng Y, Lu X, Luo J (2004) Nanoscale effect on ultrathin gas film lubrication in hard disk drive. J Tribol 126:347

Prabha SK, Sreehari PD, Murali GM, Sarith PS (2013) The effect of system boundaries on the mean free path for confined gases. AIP Adv 3:102107

Qixin L, Zhiyong C (2014) Study on the characteristics of gas molecular mean free path in nanopores by molecular dynamics simulations. Int J Mol Sci 15:12714–12730

Sharipov F (2001) Application of the Cercignani–Lampis scattering kernel to channel gas flows. AIP Conf Proc 585:347

Venna SR, Carreon MA (2009) Highly permeable zeolite imidazolate framework-8 membranes for CO_2/CH_4 separation. J Am Chem Soc 132(1):76–78

Yave W, Car A, Wind J, Peinemann KV (2010) Nanometric thin film membranes manufactured on square meter scale: ultra-thin films for CO_2 capture. Nanotechnology 21(39):395301